CONF-920124--31

Suppression of beam induced pulse shortening modes in high power RF generator TW output structures*

J. Haimson and B. Mecklenburg
Haimson Research Corporation
4151 Middlefield Road • Palo Alto, California 94303-4793

ABSTRACT

Several different style 11.4 GHz relativistic klystrons, operating with beam pulse widths of 50 ns and using large aperture, tapered phase-velocity TW structures,[1] have recently demonstrated output RF power levels in the range of 100 to 300 MW without breakdown or pulse shortening. To extend this performance into the long pulse regime (1 μs) or to demonstrate a threefold increase in output power by using higher currents, the existing TW circuit designs must be modified (a) to reduce the cavity maximum surface E-fields by a factor of 2 to 3, and (b) to elevate the current threshold values of the beam induced higher order modes (HOM) to ensure avoidance of RF pulse shortening and associated instabilities. A technique for substantially elevating this threshold current is described, and microwave data and photographs are presented showing the degree of HOM damping achieved in a recently constructed 11.4 GHz TW structure.

1. INTRODUCTION

The pulse shortening phenomenon, also referred to as beam breakup (BBU), is a beam induced higher order mode instability first observed in 1957/1958 in single section uniform impedance disc loaded TW structures used in short linacs (regenerative BBU), and subsequently encountered in a different form (cumulative BBU) in 1966[2] with multi-section linacs having identical design, nonuniform impedance TW structures. The threshold pulse current at the onset of these BBU instabilities were typically 100 to 300 mA and 10 to 20 mA for the regenerative and cumulative forms, respectively; and the instability was invariably accompanied by a beam induced large RF signal having a frequency 40 to 50% higher than the TM_{01} operating frequency of the TW structures. Both types of BBU instability, as related to electron linear accelerator structures, have been reviewed in detail and comprehensively referenced elsewhere,[3] and only a brief description is given here in order to better understand the mechanism as related to high power RF generator TW output structures designed for deceleration of high current electron beams.

1.1 Manifestation and mechanism of pulse shortening

In disc loaded TW accelerator structures, the instability is typically presented by a somewhat erratic, and continuous reduction of the width of the output beam pulse as the current is increased above a critical threshold value. The loss of full pulse width beam transmission is caused by the buildup of a TM_{11}-like mode that deflects the beam into the walls of the structure. This dipole-like mode has longitudinal E_z-field maxima of opposite polarity on either side of the axis, with zero E_z-field and maximum H_ϕ-field on axis. Also, axial components of H-field, introduced by the beam aperture fringe fields, lead to the propagation of an accompanying TE_{11}-like mode. Because of its hybrid nature, this HOM is commonly called the HEM_{11} mode, having both upper and lower branches, as shown for example in the Figure 3 dispersion diagrams of a large beam aperture ($2a \approx \lambda/2$) TW output structure for a high power 11.4 GHz RF generator. With broad band structures of this type, mode differentiation becomes more difficult, and the HEM_{11} instability resonances can approach within 15 or 20% of the TM_{01} operating frequency. As the diameter of the beam aperture is decreased, the HEM_{11} forward group velocity is reduced; and after passing through a region of duality,[4,5] the group velocity fully reverses, and the mode exhibits pure backward wave propagating characteristics, as in the majority of TW linac structures.

The transverse sweep of the beam can be explained as an instability commencing from noise (charge asymmetry) exciting an HEM_{11} resonance at an "opportunistic" frequency that establishes the most suitable phase slip ($\alpha \approx \pi$) for optimizing the beam/wave interaction, i.e., for the dipole-like mode to deflect the beam and for the beam to then transfer energy back to the mode. This occurs when electrons initially deflected from the axis, having increasing radial displacement (x) with distance traversed along the structure, slip forward on the wave to experience an increasing amplitude

*This work was supported in part by the U.S. DOE and the Lawrence Livermore National Laboratory.

FG03-92ER81285

For publication in Proceedings of the SPIE Symposium on Intense Microwave and Particle Beams III, Los Angeles, California, vol. 1629, pp. 209-219, January 1992.

DISCLAIMER

E_z decelerating field ($x\ \partial E_z/\partial x$), thereby transferring energy to the mode. This energy is reflected or propagates back to the beginning of the circuit, causing further deflection of the beam so that above a particular pulse width and threshold current, the beam induced power will exceed the losses and the HEM_{11} fields, amplified by this regenerative feedback mechanism, will produce an exponential growth of the beam deflection. The HEM_{11} mode is particularly effective in sweeping the beam into the walls of the structure, even in the presence of a strong focusing field, because the interaction typically occurs in the vicinity of the π mode (refer Figure 3), i.e., a region of high impedance, with a finite distribution of frequencies having relatively small phase shifts per cavity between the wave and the beam. Thus, a high probability exists for the excitation of a resonance that will establish a near optimum combination of beam transverse displacement and power extraction, i.e., analagous to the excitation of a klystron detuned penultimate cavity that extracts sufficient beam power for subsequent longitudinal displacement (bunching) of the beam.

A solution to the regenerative BBU problem was demonstrated in 1962 with the introduction of a series of high current, dual-section linacs using TW circuits having a constant phase shift per cavity in the dominant mode but comprised of several disc loaded, short uniform segments, of different length and impedance, interconnected with matched transitions. The HEM_{11} incoherency associated with these structures enabled an order of magnitude increase in beam current to be achieved (up to 3 A) at long pulse widths (8 to 10 μs) without evidence of BBU.[6,7]

The threshold current for regenerative BBU has been investigated[8,9] and shown to be dependent on a variety of factors including the wavelength (λ), group velocity (v_g) and phase slip of the HEM_{11} mode, the length (L), transverse shunt impedance ($r_\perp$) and Q of the structure, and the beam entry (p) and exit (p_o) longitudinal momenta. For a uniform impedance structure, the starting current (for infinite buildup time) in the absence of focusing, has been given[3,8] for TW and SW conditions as

$$I_s(TW) \approx \left(\frac{\pi}{g_2}\right)\left(\frac{v_g}{c}\right)\left(\frac{Q}{r_\perp \lambda}\right)\frac{pc}{e}\left(\frac{\lambda}{2L}\right)^3 F_a(p,p_o) \tag{1}$$

and

$$I_s(SW) \approx \left(\frac{\lambda}{2g_2}\right)\left(\frac{\pi}{L}\right)^2 \frac{1}{r_\perp}\left(\frac{pc}{e}\right) F_a(p,p_o) \tag{2}$$

where the coupling coefficient $g_2 = \frac{1}{2}(1 - \cos\alpha - \frac{1}{2}\alpha \sin\alpha)/(\alpha/\pi)^3$ has a maximum value of 1.04 when the phase slip $\alpha = 2.65$, and F_a is a correction factor to account for change in longitudinal momentum of the beam during transit of the structure.

With multi-structure systems, the buildup mechanism for cumulative BBU can be likened to an extended interaction transverse deflection amplifier, where a small transverse momentum modulation caused by an HEM_{11} resonance in an initial structure results in a progressively increasing beam displacement and a growth of the HEM_{11} field intensity in the subsequently located structures; i.e., the HEM_{11} signature is carried on the beam and excites all the subsequently located structures having identical geometry, causing coherent buildup of the HEM_{11} fields with distance and time.

Techniques that have successfully raised the cumulative BBU threshold current include, partial detuning of the structures and the use of magnetic focusing elements,[3] the use of different (groups) of structures to avoid coherence,[10] and the use of a progressive stop-band technique[11] to systematically displace the HEM_{11} dispersion diagram so that strong HEM_{11} signals carried on the beam, after interaction with upstream groups of structures, fall outside (and below) the HEM_{11} pass bands of subsequently located groups.

2. CATEGORIZATION AND PERFORMANCE OF DISC LOADED TW OUTPUT CIRCUITS

Although linac and RF generator disc loaded TW output structures have many features in common, HEM_{11} mode interaction with high perveance and high emittance beams of rapidly decreasing energy introduce additional considerations that are uniquely related to RF generator TW output circuits and their specific application. The 100 to 300 MW output power TW disc loaded structures discussed in this paper can be separated into two broad design categories:

(a) moderately slow wave circuits ($0.6c < v_p < c$) having constant or tapered phase velocity (v_p) characteristics and designed to operate with electron beams of, say, 400 to 1000 keV and up to approximately 500A, and

(b) structures designed to operate with beam energies of, say, 1 to 5 MeV with source currents of 1000A (or greater), and using essentially $v_p = c$ circuits, with appropriate phase adjustment to compensate for space charge effects.

Design and performance characteristics of 11.4 GHz TW output structures representing both of the above categories are shown listed in Table I, with associated references describing technical details and performance data. (A third category of TW output structure, not discussed here, has been used to generate intense short bursts of RF power at S-band, with 10 to 20 MeV, 10-20A, electron linac beams.[12,13])

TW structures in the first category, designed typically for relativistic klystron applications using axial magnetic fields in the range of 0.3 to 0.6T, have inherently high values of HEM_{11} threshold current, and BBU has not been encountered in single structures operating in the short pulse regime (50 ns), even though HEM_{11} resonances have been observed.[14,15] (Also, Russian workers have observed parasitic oscillations, recently reported as not attributable to HEM_{11} pulse shortening, in a 14 GHz high gain relativistic klystron[16] that uses a 7 cm long, $v_p = 0.9c$ uniform TW structure with an output of 50 to 60 MW and an electron beam pulse of approximately 150 A at 1 MeV and 700 ns.)

The output structures referenced in Table I for the SHARK/MOK-2 experiments and the HRC-X791 50 dB gain, TW relativistic klystron are typical examples of slow wave circuits in the first category. These early configuration (1987/1988) slow wave structures, designed for high current (500 A) relativistic beam interaction, introduced the concept of trading-off shunt impedance against circuit length by adopting very large beam apertures ($2a \approx \lambda/2$) so that high levels of peak RF power could be extracted without exceeding the output circuit E-field breakdown value. Additional important attributes were the ultra-fast RF filling time (≈ 1000 ps) with attendant phase insensitivity to normal temperature and frequency variations, and the simplicity with which these X-band structures could be designed and tuned to control the rapid buildup of intense space charge debunching fields (> 100 kV/cm) during the final stage of beam deceleration - an important prerequisite for demonstrating maximum RF conversion efficiency. For example, the HRC-X791 TW klystron shown in Figure 1 comprises three gain cavities and a combined bunching and TW output assembly that uses a graded axial magnetic field distribution[1] to achieve an output power of 100 MW with an RF conversion efficiency of approximately 43 percent. Advantage was taken of this short pulse application (50 ns) to design the output cavity with a relatively high surface maximum E-field of 110 MV/m at 100 MW. (In this short pulse regime, the highest surface E-field experienced to date with these 11.4 GHz TW structures is the 150 MV/m value listed in Table I for SHARK at 300 MW.)

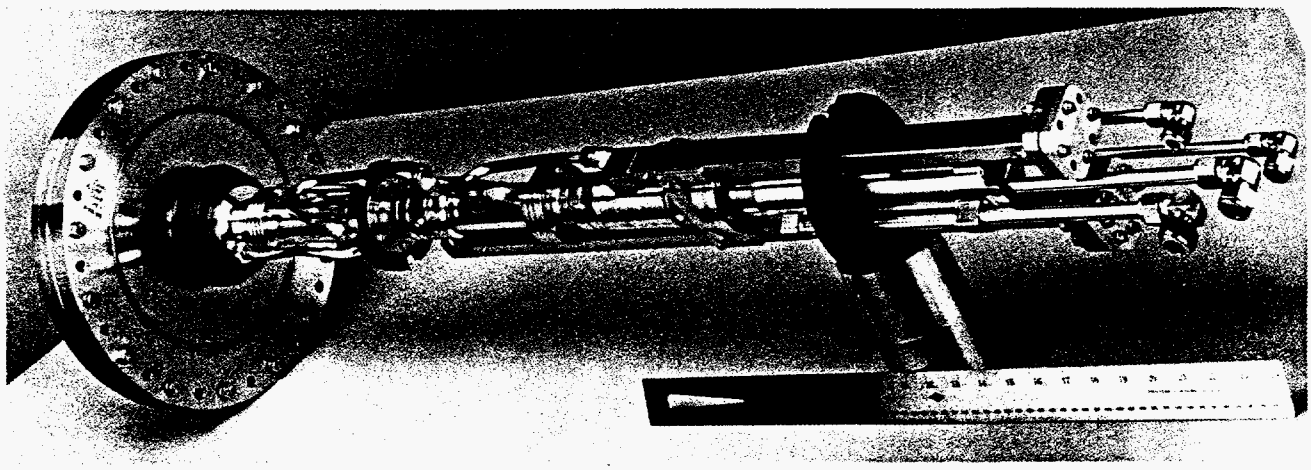

Fig. 1. HRC-X791 100MW, 50 ns, 11.4 GHz TW Output Klystron Designed for Use with a Small Bore (10 cm ID) Precision Aligned Solenoid. Max. Repetition Rate = 1000 pps.

TABLE I

DESIGN AND PERFORMANCE CHARACTERISTICS OF 11.4 GHz TW OUTPUT STRUCTURES

TW Design No.	TW Output Structure Application and Reference	Electron Source V_o (MeV)	Demonstrated Output Power P_o (MW)	Number Active Cavities ($2\pi/3$ Mode)	Tapered Beam Apertures and/or Phase Velocity	HOM Damping Circuit	RF Power Gain* (dB)	Output Cavity Parameters		
								Beam Aperture (in)	Shunt Impedance (MΩ/m)	Surface E_{max} at P_o (MV/m)
1	SHARK/MOK-2[1,17]	1.1 - 1.3	300 (No BBU)	6	Yes	No	15.2	0.552	31	152
2	Choppertron[18,19]	2.5 - 2.7								
	TW1		240	6	No	No	15.5	0.552	46	132
	TW2		180 (BBU Limited)	6	No	No	15.5	0.552	46	114
3	TW Klystron[1,15] (HRC-X791)	0.45 - 0.5	100 (No BBU)	5	Yes	No	11.6	0.512	NR	110
4	Choppertron[20] TW3	2.5 - 2.7	120 (No BBU)	4	No	Yes	11.8	0.512	54	80
5	Choppertron TW4**	2.5 - 2.7	(Objective) 500	4	No	Yes	12.5	NR	46	107

*RF Power Gain = (Final Cavity Output/First Cavity Output)

**New design proposal

As embodied in the TW structure designed to replace the standing wave output circuit for the SHARK experiments,[14] the first two cells of the X-791 TW output structure were also fabricated with surface contoured, low carbon 304 stainless steel components that were pretuned and then hydrogen furnace brazed to the main body of the structure using copper-gold alloy. These slow wave structures were designed with side wall coupled, offset body output cavities to minimize field asymmetry; and with exception of the SST cavities, no HOM absorption or extraction circuits were incorporated into these particular assemblies because the natural incoherency of the nonuniform structure was sufficient to elevate the BBU threshold current well above (>1000 A) the application requirements. (The authors strongly recommend avoiding uniform geometry when using such TW structures for very high current or long pulse applications.)

TW structures in the second category can have substantially reduced values of BBU threshold current, especially if operated in a multiple array as required, for example, in a Two Beam Accelerator application.[21] Even with short pulse operation, TW circuits used in high current (1000 A), multiple structure applications will, in general, require heavy suppression of the HEM_{11} fields if pulse shortening due to both regenerative and cumulative BBU is to be prevented.

The choppertron $v_p=c$ circuits (refer TW1 and TW2 in Table I) are typical examples of the second category of TW output structure. The prototype version of this RF generator made use of two contiguously installed (refer Figure 2) identical geometry, uniform impedance TW output circuits that were designed and fabricated without HOM suppression;[1] i.e., no attempt was made to elevate the BBU natural threshold. With a 50 ns beam and an axial magnetic field of approximately 0.25T, pulse shortening was observed in the second structure at an unmodulated threshold current of approximately 600 A.[19] The total output power, limited by pulse shortening, was 420 MW. A HOM damped output structure (TW3) incorporating an HEM_{11} suppression circuit, as discussed in Section 4 below, was fabricated and tested[20] to investigate its effectiveness in overcoming multi-structure pulse shortening and to evaluate the possibility of operating at higher currents to achieve higher power levels.

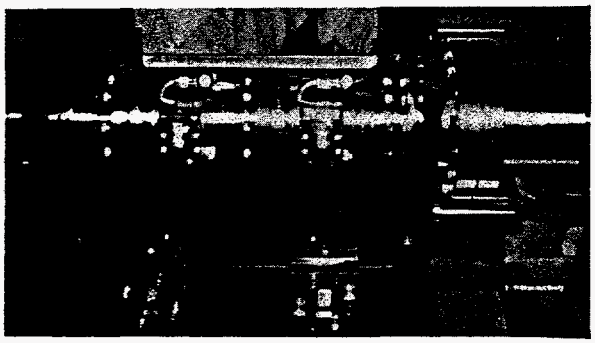

Fig. 2. View of Choppertron Dual Output Disc Loaded TW Structures.

The recently proposed 11.4 GHz output structure listed as TW4 in Table I is a HOM damped high current structure conservatively rated for 1000 A, 50 ns operation to give an output power of 500 MW at a surface maximum E-field of 107 MV/m. For long pulse operation using a 550 A, 1 μs beam, this TW structure is designed to give an output power of 150 MW with a surface maximum E-field of only 59 MV/m.

3. HEM_{11} PULSE SHORTENING CONSIDERATIONS

Even though average beam energies associated with TW output structures can be two orders of magnitude lower than in short TW linacs, the natural threshold currents for regenerative BBU can be approximately three orders of magnitude higher. This is due to a variety of mitigating factors, especially the marked reduction of circuit length (normalized to the HEM_{11} wavelength), the higher group velocities and lower $(r/Q)_\perp$ values associated with the larger beam apertures, and the much larger betatron phase shifts that occur per HEM_{11} wavelength in a TW output structure. For example, during the final stages of deceleration in the X-791 output structure, [even with the axial magnetic field graded from 0.45 to 0.3T to optimize RF output power], the betatron phase shift is $\approx\pi$ per HEM_{11} wavelength, and lower energy particles radially deflected initially from the centerline will return to the axis after traversing a distance of only 2 cm; i. e., the HEM_{11} mode deflected particles experience a considerable azimuthal displacement with respect to the direction of the initial transverse momentum vector. Thus, beam interaction with the radially polarized HEM_{11} E_z fields is reduced, both by the azimuthal displacement and the reduced deflection of the decelerating electrons in the strong axial magnetic field, and this can result in a substantial elevation of the BBU threshold current.

Equation (1) can be used to make a rough estimate of BBU threshold current by comparing a large aperture, 5 cm long 11 GHz uniform impedance TW output structure and a loaded 18 MeV 3 meter S-band uniform impedance section, $2a=\lambda_o/5$, (Darmstadt linac[7]) having a BBU threshold current of 0.18 A, by applying the ratios of 6 for the HEM_{11} group

velocity, 1/3 for $(r\lambda/Q)_\perp$, 1/100 for the longitudinal momenta, 1/18 [=(5/2.2)(7.1/300)] for the structure length normalized to the HEM_{11} wavelength (L/λ), and $\approx(\pi/2)^2$ for the effects of strong focusing. This comparison gives 460 A as a crude estimate of the BBU threshold for the short structure assuming similar phase slip coupling coefficients in both circuits.

An accurate estimate of the coupling coefficient and effective interaction length can be obtained from a knowledge of the BBU frequency and dispersion characteristics of the structure. Typical ω/β characteristics for a 3 cell per wavelength, TW structure designed for $v_p=c$ operation at 11.4 GHz and having a beam aperture of $2a\approx\lambda/2$ are shown plotted in Figure 3. It can be noted that, unlike typical TW linac structures, all three of the higher mode pass bands shown plotted above the dominant mode exhibit forward propagating characteristics and, of considerable importance for mode suppression, the HEM_{11} lower branch zero mode cutoff is actually 450 MHz lower than the TM_{01} operating frequency, causing the two passbands to partially overlap. Also, the beam induced HEM_{11} BBU frequencies observed with these structures at approximately 13.5 to 13.7 GHz are consistent with the $v_p\leq c$ intercepts on the HEM_{11} lower branch where, for the near π mode resonances, phase slips of 20 to 30° per cell in the six cell circuit result in a near maximum value for the phase slip coupling coefficient.

Figure 3 also shows that the BBU frequency is only 20% higher than the TM_{01} operating frequency, and that there is a high probability of exciting backward space harmonics in both the HEM_{11} upper branch and the HEM_{21} (quadrupole) lower branch (17½ to 18½ GHz). Although the $r_\perp/Q$ values associated with these higher modes are low compared to the HEM_{11} lower branch, for multi-structure high current applications, it was thought desirable to extend the bandwidth of the HOM suppression circuitry to include these higher frequencies. For large aperture circuits, variations of the aperture diameter cause large changes in the HEM_{11} lower branch zero mode cutoff frequency,[4,23] but the $v_p=c$ intercepts always remain in close proximity to the π mode cutoff frequencies, suggesting that given sufficient drive, without suppression, HOM pulse shortening could be experienced with all of these circuits. In this regard, the use of large aperture circuits is favorable because, for TW output structures, unlike linacs, reduced longitudinal shunt impedance is often the design goal (to allow circuit extension), and this also results in a substantial reduction in transverse shunt impedance and $r_\perp/Q$.[22,23] Typically, doubling the aperture diameter can cause a 3:1 reduction in unit length $r_\perp/Q$ which assists directly in elevating the BBU threshold. The group velocity and $r_\perp/Q$ values used for the Figure 3 structure HEM_{11} mode lower branch BBU calculations were 0.12 c and 20 Ω/cm, respectively.

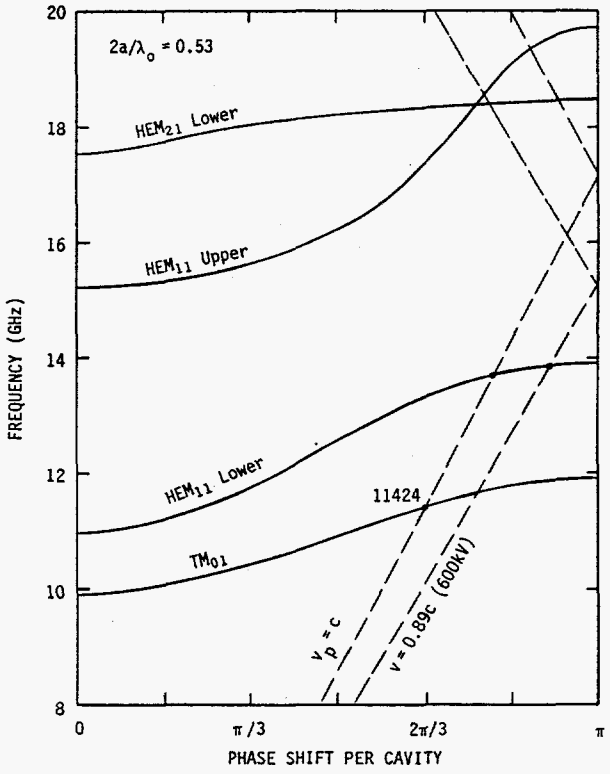

Fig. 3. Dispersion Diagram of a Large Beam Aperture Disc Loaded Structure.

In TW relativistic klystrons, it is advisable that the TW structure input drift tube be designed to prevent HOM signals from propagating back along the beam tube. Thus, instead of a TW interaction, the HEM_{11} fields may buildup resonantly due to a trapped SW between the input cutoff drift tube and a mismatch presented at the output of the circuit. In this event, BBU growth will simply be dependent on the beam induced power exceeding the circuit losses. Under these circumstances, improving the output coupler match is highly desirable, and consideration should also be given to the accompanying orthogonally polarized HEM_{11} degeneracy. On the other hand, the use of HEM_{11} cutoff drift tubes may not be practical for a multiple array of output structures using a high emittance large diameter beam; and in this case, HEM_{11} field buildup can be expected due to a combination of both TW regenerative and cumulative BBU mechanisms. It is the need to heavily suppress these BBU mechanisms in multi-structure applications that is addressed below.

Figure 4 shows the high current impulse response results of cumulative BBU deflection amplification computations[3,24] for a dual output structure assembly (Choppertron TW1 and TW2) using identical geometry circuits separated by 12½ cm and compares BBU deflection amplification factors $<x/x_o>$ for structures having HEM_{11} Q values of 500 (propagation losses only) and 10 (special suppression) using a 400 A beam and entry and exit beam energies of 2.7 and 0.7 MeV, respectively. Initial beam offsets (x_o) of 0.1 and 0.2 mm were assumed, and strong focusing was applied in all cases. Initial conditions assumed a noise amplitude of 10^{-5} cm; thus, with an 8 mm beam in a 14 mm aperture, noticeable beam interception will commence at a deflection amplification of $\approx 4\times10^4$ with a major loss of beam occurring at $<x/x_o> \approx 10^5$. A trapezoidal beam pulse was assumed having a rise time of 5 ns; and the HEM_{11} frequency and $R_\perp/Q$ values used were 13.70 GHz and 110 Ω, respectively. The Figure 4 data indicates that with two undamped circuits, BBU can occur before the 50 ns beam pulse has terminated, and that an extremely low Q is necessary to avoid pulse shortening.

The Figure 5 BBU amplification curves are the predicted results for operation of four series connected uniform impedance structures, each with heavily damped (Q=10) HOM resonances, compared with Q=500 undamped structures. An entry beam of 400 A at 4.8 MeV was used; intersection spacing was maintained at 12.5 cm; and the exit energy was 0.8 MeV. Beam offset examples of 0.1 and 0.2 mm were assumed for all structures, and strong focusing was again applied. These results again confirm the necessity for extremely low Q values, and also reveal that, if contemplating the use of four output structures, a further reduction in the BBU amplitude factor would be prudent. This reduction can be readily achieved, with the same technique as used in linacs, by introducing incoherency into some of the structures, e.g., by altering the dimensions of the disc aperture, thickness or spacing. The lower amplitude curve in Figure 5, for Q=10 and an offset of 0.2 mm, shows the effect of reducing $R_\perp/Q$ to 55 Ω.

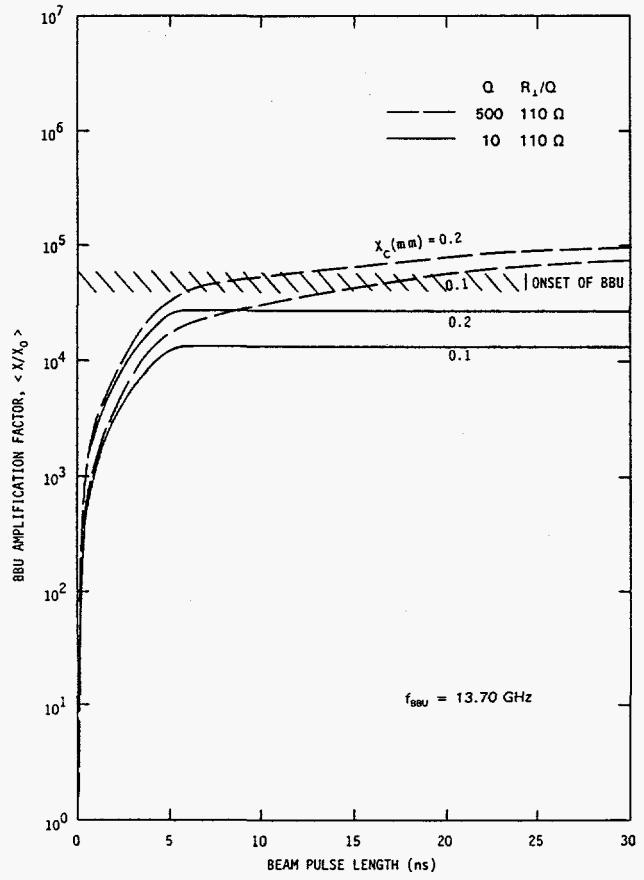

Fig. 4. Comparison of BBU Deflection Amplification using Two Uniform Impedance Output Structures with and without HOM Suppression. (V_o = 2.7 MeV and I = 400 A.)

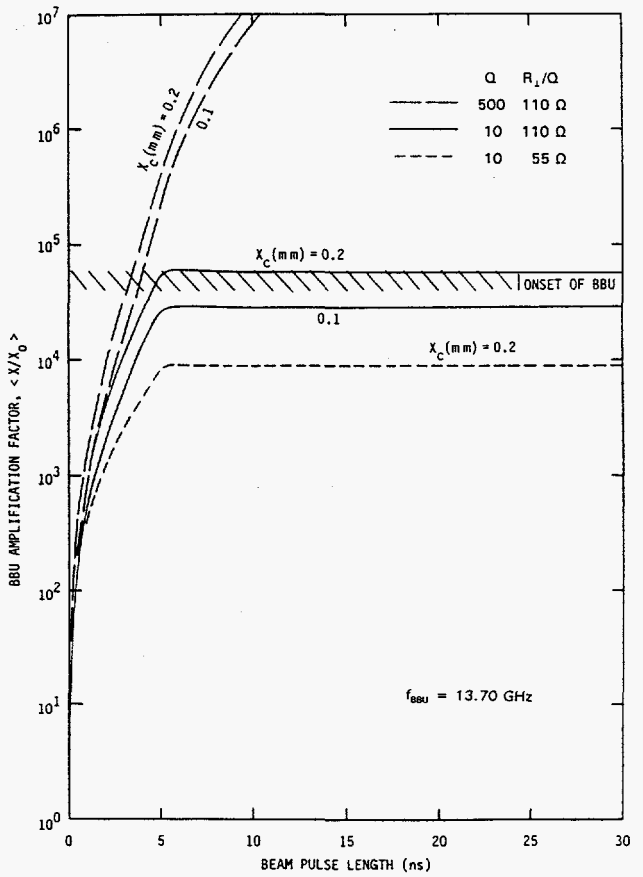

Fig. 5. Comparison of BBU Deflection Amplification using Four Output Structures with and without HOM Suppression. (V_o = 4.8 MeV and I = 400 A.)

4. HEM_{11} SUPPRESSION AT HIGH CURRENT LEVELS

The BBU analyses indicated that multi-section high current operation of TW output structures required local heavy suppression of the traveling dipole field patterns and suggested that loaded Q levels of ≤ 10 would be necessary. The suppression circuit chosen for this application evolved from earlier work associated with development of a long pulse relativistic klystron and with large aperture, disc loaded TW structures used for cw operation with pulse stretcher rings. These cw structures were designed to transfer and/or extract energy from a recirculating high energy beam that made several thousand passes through the disc loaded circuit during the system interpulse period of a few milliseconds. Thus, agressive anti-BBU precautions were necessary, and a broad mix of HOM de-Q-ing techniques were used,[22] including incoherency, differential extraction, and absorption. In addition to the use of tunable, large diameter ($2a \approx \lambda/2$), RF lossy input and output beam drift tubes containing extraction probes, the HEM_{11} power was channelled out of these S-band cw structures using HOM extraction offset coupling cavities and broad band matched external rectangular waveguide assemblies. These radially attached orthogonally disposed HOM terminating waveguides were oriented azimuthally at 45° to the dominant mode high power coupling apertures (TM_{01}/TE_{10}) to provide additional de-Q-ing for both HEM_{11} mode polarizations. The damping afforded by these various extraction techniques (Q-s of several hundred), together with reduced values of coupling coefficient and effective interaction length, although adequate for the pulse stretcher application, needed further extension to satisfy the RF generator multi-structure requirement for an additional two orders of magnitude reduction in Q. Moreover, installation of the RF generator 11 GHz TW output structures in a relatively small diameter solenoid assembly required a far more compact layout for the broad band HOM terminations than the previously developed system.

The above requirements were satisfied by developing an azimuthally folded waveguide configuration that enabled two pairs of diametrically opposed HOM extraction channels to be machined back-to-back in an integral dual cell stainless steel assembly that was located at the input end of the TW output structure. The Figure 6 X-ray reveals the layout concept of this 4-port HOM extraction circuit and shows the folded waveguide channels prior to installation of the terminations.

Fig. 6. Radiograph of HOM Suppression Circuit Cold Test Model Showing the 4-Port Folded Waveguide Concept.

This HOM folded circuit arrangement made effective use of the unoccupied space close to the centerline; provided extra length by azimuthal extension so that the terminations in each channel could be conveniently broad-banded (greater than an octave); prevented line of sight exposure of the terminations to the beam; provided Q values ≈ 10; allowed existing assembly, water cooling and tuning procedures to be maintained; and enabled the azimuthal orientation of the HOM extraction channels to be selected to suit a particular application. For example, with the choppertron system, the first TW structure is positioned against the chopping collimator,[18] and the entry beam retains a small transverse momentum component polarized essentially in the direction of the vertical RF sweep. Thus, for this application, the HOM supression circuit, which was to be located alongside the chopper collimator, had the extraction channels azimuthally biased to increase the acceptance of vertically polarized field patterns, as indicated in Figure 6.

The Figure 7 photographs of the choppertron damped structure (TW3) show the copper cavity brazed sub-stack, the folded circuit stainless steel HOM suppression assembly and the high power WR90 RF output flange.

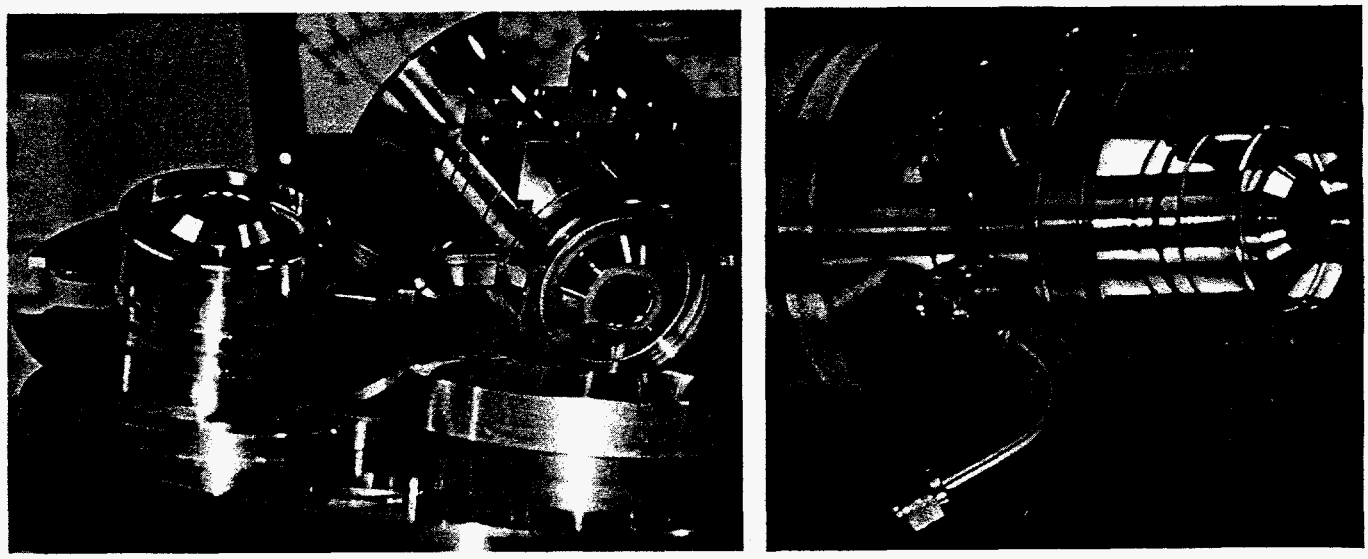

Fig. 7. 11.4 GHz HOM Damped Output Structure During Final Assembly.

Cold test data obtained from undamped and HOM damped TW structures having similar geometry are compared in Figures 8 through 10. Figure 8 shows the response from each structure using a detector located on the WR90 horizontal output arm, and a 12-18 GHz swept signal introduced at the beam entry port with an E-probe positioned 3 mm off-axis and in the plane of the WR90 output arm. The first and second set of resonances are representative of the HEM_{11} lower and upper branches, respectively; and the comparison shows that the "vertically biased" HOM suppression circuit is effective in damping the horizontally polarized BBU dipole fields.

Figures 9 and 10 compare beam centerline propagation characteristics of the undamped and HOM damped structures for different polarization planes.

In Figure 9, off-axis E-probes, located on diametrically opposite sides of the centerline and in the plane of the WR90 output arm, were used at the beam input and output ports for excitation and detection, respectively. The centerline transmitted signals of the undamped structure were complementary to the Figure 8 data, and confirmed that, for this polarization, the HEM_{11} lower branch resonances were effectively coupled (magnetically) out of the WR90 port and that a broad range of HEM_{11} upper branch (TE_{11}-like) resonances were not. The centerline transmitted signals of the damped structure show

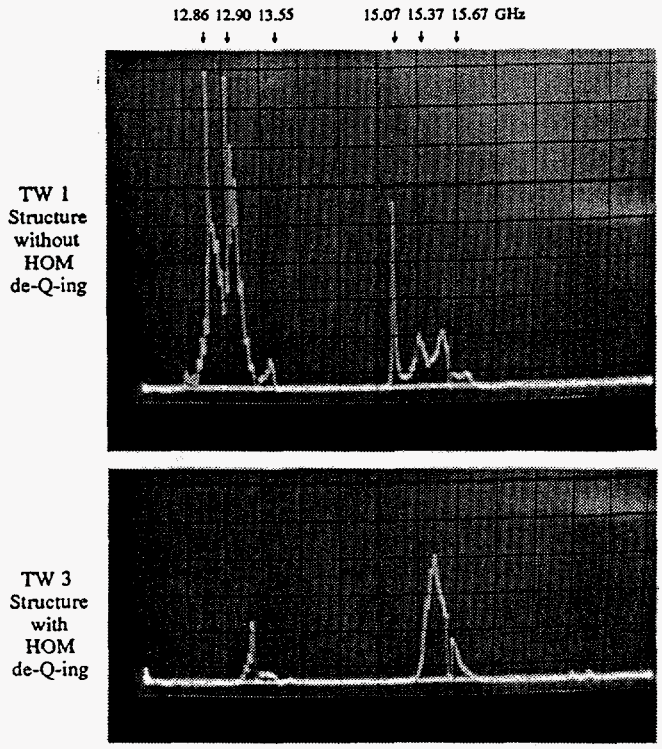

Fig. 8. 12-18 GHz Frequency Sweep of 11.4 GHz TW Circuits Showing the Effects of HOM Damping. RF Signal Introduced with a Beam ℄ Input Off-Axis E-Probe in the Plane of the Output WR90 RWG and its Terminating Coaxial Adaptor and Detector, with Beam ℄ Exit Aperture Unperturbed.

a very low residual transmission of the HEM_{11} lower branch frequencies and the effective suppression of all but one (15.3 GHz) of the HEM_{11} upper branch resonances.

The Figure 10 data were recorded under similar conditions to Figure 9 except the off-axis E-probes were rotated 90° with respect to the plane of the WR90 output arm. The undamped structure data now show strong HEM_{11} lower branch signals freely transmitted along the centerline (because coupling through the WR90 port is inhibited with this polarization); and the damped structure, with its HOM extraction circuitry now optimally aligned with the vertically polarized signal, appears to have effectively suppressed the beam centerline transmission of all the launched HEM_{11} modes. This type of heavy damping at the input to a TW circuit can result in additional termination losses at the dominant mode frequency and, while beneficial for stabilizing the RF performance, will, in general, require a design compromise between degree of damping and final choice of structure length.

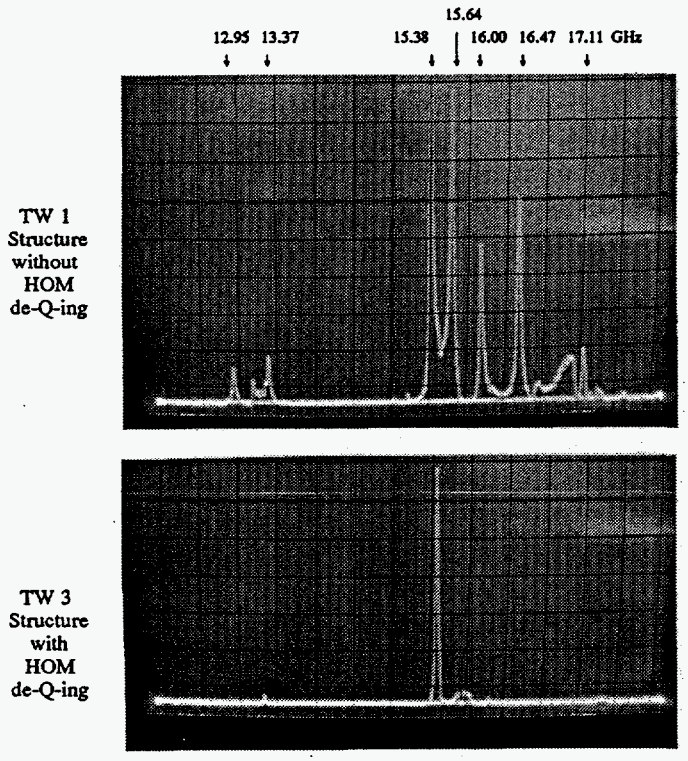

Fig. 9. 12-18 GHz Frequency Sweep of 11.4 GHz TW Circuits Showing the Effects of HOM Damping. RF Signal and Detector Off-axis E-Probes Located at the Beam ℄ Input and Output, respectively, in the Plane of the Output WR90 RWG.

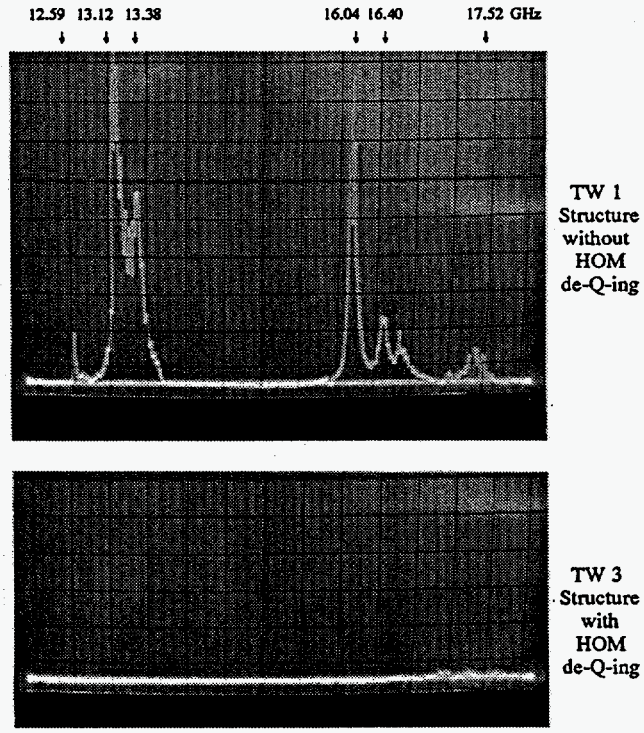

Fig. 10. 12-18 GHz Frequency Sweep of 11.4 GHz TW Circuits Showing the Effects of HOM Damping. RF Signal and Detector Off-axis E-Probes Located at the Beam ℄ Input and Output, respectively, in the Plane Orthogonal to the Output WR90 RWG.

The results of the choppertron initial high power tests using this prototype HOM damped structure (TW3) are presented in a companion paper[20] at this conference.

5. ACKNOWLEDGEMENTS

The authors would like to acknowledge the support and cooperation of the LBL/LLNL staff during the course of these investigations, and colleagues at HRC for their dedicated efforts in the design and construction of these high power TW structures.

6. REFERENCES

1. J. Haimson and B. Mecklenburg, "Use of TW Output Structures for the Generation of High Peak RF Power," Proc. of the 1990 Linear Accelerator Conference, LA-12004-C, Albuquerque, New Mexico, pp. 244-246, 1990.

2. W.K.H. Panofsky, "Transient Behavior of Beam Breakup," TN-66-27, Stanford Linear Accelerator Center, Stanford,California, 1966.

3. R.H. Helm and G.A. Loew, Chapter B.1.4, "Beam Breakup," Linear Accelerators, Eds. P. Lapostolle and A. Septier, pp. 173-221, North Holland Publishing Co., Amsterdam, 1970.

4. G. Saxon, T.R. Jarvis and I. White, "Angular-dependent Modes in Circular Corrugated Waveguide," Proc. IEE (London) 110 No. 3, pp. 1365-1373, 1963.

5. M. Bell, P. Bramham and B.W. Montague, "Pulse Shortening in Electron Linear Accelerators and E_{11} Type Modes," Nature, 198 No. 4877, pp. 277-278, 1963.

6. J. Haimson and I. Brodie, "High-Current Cathode for Electron Linear Accelerator," Nature, 199 No. 4895, pp. 795-797, 1963.

7. J. Haimson, "High Current Traveling Wave Electron Linear Accelerators," IEEE Trans. Nucl. Sci., NS-12 No. 3, pp. 996-1011, 1965.

8. P.B. Wilson, "A Study of Beam Blow-up in Electron Linacs," Internal Memorandum HEPL-297, 1963.

9. E.L. Chu, "A Crude Estimate of the Starting Current for Linear Accelerator Beam Blowup in the Presence of an Axial Magnetic Field," TN-66-17, Stanford Linear Accelerator, Stanford, California, 1966.

10. H. Leboutet, "Auto-deflexion du Faiscean d'un Accélératur Linéaire," Internal Report INT. 2217-HL, CSF, France 1966.

11. Linear Accelerators, op. cit. Chapter B.3.2, p. 450.

12. US Patent 3,343,101.

13. D.G. Dow et al, "Pulse Compression using Linear Accelerator Techniques," Conference on Electron Device Research, Cornell University, 1964.

14. M.A. Allen et al, "Relativistic Klystrons," Proc. of the 1989 IEEE Particle Accelerator Conference, 89CH2669-0, pp. 1123-1127, 1989.

15. D.L. Goodman and B.G. Danly, "Induction Linac Driven Relativistic Klystron and Cyclotron Auto-resonance Maser Experiments," SPIE Conf. on High Power Microwave Sources, Los Angeles, 1991.

16. V.E. Balakin et al, "Experimental Research on the Relativistic Klystron for VLEPP," Presented at the Third Intl. Workshop on Linear Colliders, Protvino, Russia, 1991.

17. G.A. Westenskow et al, "Relativistic Klystrons for High Gradient Accelerators," Proc. of the 1990 Linear Accelerator Conference, LA-12004-C, Albuquerque, New Mexico, pp. 192-194, 1990.

18. J. Haimson and B. Mecklenburg, "Design and Construction of a Chopper Driven 11.4 GHz Traveling Wave RF Generator," Proc. of the 1989 IEEE Particle Accelerator Conference, 89CH2669-0, pp. 243-245, 1989.

19. G. Westenskow et al, "A Chopper Driven 11.4GHz Traveling-Wave RF Generator," Proc. of the 1991 IEEE Particle Accelerator Conference, 91CH3038-7, pp. 646-648, 1991.

20. T.L. Houck et al, "Relativistic Klystron Research for Two-Beam Accelerators," Proc. of the SPIE's International Symposium on Lasers, Sensors and Spectroscopy, vol. 1629-47, 1992.

21. A.M. Sessler and S.S. Yu, "Relativistic Klystron Two Beam Accelerator," Phys. Rev. Lett., 58, p. 2439, 1987.

22. J. Haimson and B. Mecklenburg, "A CW Non-synchronous Traveling Wave Structure for a 300 MeV Pulse Stretcher Ring," Proc. of the 1987 IEEE Particle Accelerator Conference, 87CH2387-9, pp. 1919-1921, 1987.

23. J.W. Wang and G.A. Loew, "HEM_{11} Modes Revisited," Proc. of the 1990 Linear Accelerator Conference, LA-12004-C, Albuquerque, New Mexico, pp. 135-137, 1990.

24. J. Haimson, B. Mecklenburg and C. Williamson, "Comparison of Conventional L and S-Band Electron Linacs as Pion Sources Suitable for Radiotherapy," IEEE Trans. Nucl. Sci., NS-22 No. 3, pp. 1805-1808, June 1975.